Materials Chemistry and Physics 215 (2018) 69–80

Contents lists available at ScienceDirect

Materials Chemistry and Physics

journal homepage: www.elsevier.com/locate/matchemphys

Surface modified alginate multicore microcapsules and their application in self-healing epoxy coatings for metallic protection

Iee Lee Hia[a], Weng Hoong Lam[b], Siang-Piao Chai[c], Eng-Seng Chan[c], Pooria Pasbakhsh[a,*]

[a] Mechanical Engineering Discipline, School of Engineering, Monash University Malaysia, Jalan Lagoon Selatan, Bandar Sunway, 47500 Selangor, Malaysia
[b] Department of Chemical Engineering, Xiamen University Malaysia, Jalan Sunsuria, Bandar Sunsuria, 43900, Sepang, Selangor, Malaysia
[c] Chemical Engineering Discipline, School of Engineering, Monash University Malaysia, Jalan Lagoon Selatan, Bandar Sunway, 47500, Selangor, Malaysia

HIGHLIGHTS

- Epoxy is encapsulated within alginate biopolymer as self-healing microcapsules.
- Electrospraying and air atomization produce different capsule sizes.
- Chitosan coating improves capsules integrity and elastic modulus.
- Halloysite nanotubes increase capsules thermal properties and elastic modulus.
- Self-healing epoxy coatings show good sign of scratch healing.

GRAPHICAL ABSTRACT

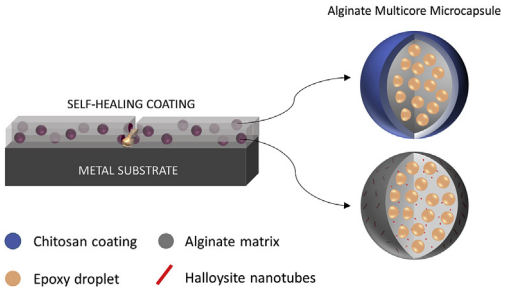

ABSTRACT

Conventionally, self-healing microcapsules are synthesized from synthetic polymers associated with complicated fabrication process. It appears in the range of (10–400 μm) to suit different applications. Here, we report green self-healing microcapsules synthesized from alginate biopolymer. The synthesis process is straightforward, require no pH and temperature change. Using simple methods (electrospraying and air atomization), alginate/epoxy microcapsules of two size range (~350 μm and ~150 μm) are fabricated. However, the smaller air atomized microcapsules collapsed after drying. Chitosan coating successfully provides structural support to small air atomized microcapsules and improves the elastic modulus of both microcapsules. Peak force quantitative nanomechanical mapping (PFQNM) under atomic force microscopy (AFM) is used to acquire the capsules elastic modulus. Chitosan coating slightly improved the elastic modulus of electrosprayed microcapsules from 3.43 ± 0.80 GPa to 4.45 ± 0.80 GPa. Although HNTs are unable to enhance the structural integrity of small microcapsules, it improves the elastic modulus of big microcapsules up to 6.04 ± 0.20 GPa. To evaluate the self-healing ability, these microcapsules and Scandium (III) triflate catalyst are incorporated into epoxy coating and applied on a metallic substrate. The capsule-catalyst self-healing coatings showed good self-healing performance in closing the gaps on the scratch.

Abbreviations: PFQNM, peak force quantitative nanomechanical mapping; AFM, atomic force microscopy; HNTs, halloysite nanotubes; Sc(OTf_3), Scandium (III) triflate; AG/EPX, alginate/epoxy; DETA, diethylenetriamine; FTIR, Fourier transform infrared spectroscopy; SEM, scanning electron microscope

* Corresponding author.
E-mail addresses: hia.iee.lee@monash.edu (I.L. Hia), wenghoong.lam@xmu.edu.my (W.H. Lam), chai.siang.piao@monash.edu (S.-P. Chai), chan.eng.seng@monash.edu (E.-S. Chan), pooria.pasbakhsh@monash.edu (P. Pasbakhsh).

https://doi.org/10.1016/j.matchemphys.2018.05.021
Received 19 January 2018; Received in revised form 26 April 2018; Accepted 12 May 2018
Available online 14 May 2018
0254-0584/

1. Introduction

Self-healing composites have been a prominent research area of interest for the past two decades. These advanced materials either utilize extrinsic or intrinsic self-healing to restore the damages within composite structures. Under extrinsic self-healing, often microcapsule or vascular-network are used as the containers for the healing agents [1–5]. Monomer/catalyst and monomer/hardener are the most common self-healing systems. The first one consists of catalysts that trigger the polymerization of the monomer for healing such as Grubbs [6], Tungsten Chloride (VI) [7], Scandium (III) triflate [8] and Hoveyda 1st Grubbs catalyst [9]. The second system utilizes monomer and hardener including epoxy/thiol [10], epoxy/amine [11] and isocyanate/thiol [12] as the self-healing agents. In contrast, intrinsic self-healing engages reversible bonding such as dynamic covalent [13] and Diels-Alder [14] to restore the broken polymer structure.

Amongst, capsule-based self-healing system is preferred as it is easily blended into the current applications without altering the chemical structures of the matrix. The common application includes self-healing coatings for corrosion prevention in metal substrates [15–18]. Metals have been existed for the past centuries, appeared in construction materials, transportations to consumer goods. In past, chromate conversion coating was applied on metals to prevent oxidation/corrosion. However, the toxicity and carcinogenic properties of chromium have lead for more environmental friendly approaches [19]. To date, microcapsules containing linseed oil [16], Tung oil [20], hexamethylene diisocyanate (HDI) [15], mixture of triazole and oleate derivatives [21], epoxy and amine [22], siloxane and catalyst [23] were reported. These microcapsules were mixed into coating matrix and spread on top of a metal substrate. Whenever a crack emerges, the healing agents will be released from the ruptured capsules and seal the damage, preventing the metal substrate underneath being corroded.

The conventional self-healing microcapsules were mainly synthesized from synthetic polymers, including polyurea-formaldehyde, polyurethane/urea-formaldehyde, and poly(melamine-formaldehyde), where the capsule size ranges from 10 to 200 μm [24]. Our previous studies demonstrated that for the first time, non-toxic organic alginate biopolymer could be used as the encapsulating material for epoxy resin. These microcapsules were designed to have multicore internal structures that led to multiple healing ability [2]. However, the average capsule size of 320 μm achieved through electrospraying method is not suitable for thin coating applications and at the same time, higher surface area to volume ratio microcapsules is preferred for not deteriorating the mechanical properties of the self-healing composites.

Alginate biopolymer, which is derived from brown seaweed, has been widely used as encapsulating matrix for living cells, pharmaceutical drugs and scaffold for tissue engineering [25,26]. To date, most of the studies focused on utilizing gel-like structure alginate beads associated with water content of more than 95% [27]. These soft gel beads are susceptible to disintegration especially in the harsh environment; thus the beads are normally modified to enhance the structural properties [28]. Polyelectrolyte complexes have been applied widely in drug delivery systems, forming complexes between two opposite charge polyelectrolytes [29]. For instance, chitosan as the polycation polymer can bound onto negatively charged alginate surface, providing mechanical support as well as reducing the capsule permeability [30]. It can be coated on alginate beads either through dropping alginate solution into chitosan/calcium chloride solution or incubating alginate beads into chitosan solution, where the latter method provides higher chitosan adhesion [31].

Extensive studies have been done on incorporating nano-fillers such as halloysite nanotubes (HNTs) into the polymer matrix to enhance their mechanical, thermal and morphological properties [32–35]. HNTs are natural occurring aluminosilicates ($Al_2Si_2O_5(OH)_{4.n}H_2O$) with hollow tubular structures [36]. The size of HNTs ranges from 1 to 15 μm in length and 10–150 nm in diameter and the elastic modulus of HNTs is found to be 140 GPa [37]. Due to the weak hydroxyl and siloxane groups on the HNTs surface, there are relatively easy to be dispersed in non-polar polymers [38]. HNTs have been added into different polymers such as polylactide, alginate, and chitosan [27,35,38]. Most of the studies showed that adding of HNTs have successfully improved the mechanical and thermal properties of the composite. Thus, incorporating HNTs into alginate shell matrix has the potential to improve the elastic modulus of the capsules and concurrently acting as reinforcement to the composite structure.

In this work, we aimed to enhance the structural integrity and mechanical properties of alginate/epoxy (AG/EPX) microcapsules through chitosan coating and incorporation of HNT nanofillers into alginate matrix. Two ranges of microcapsule size were fabricated, i.e. 250–350 μm and 50–150 μm, to suit different applications. Their respective properties such as size, surface morphology, thermal properties, core content, chemical properties, elastic modulus of the capsules and self-healing ability as a coating were assessed. Peak Force™ Quantitative Nanomechanical Mapping (QNM) through Atomic Force Microscopy (AFM) was used to study the elastic modulus of the microcapsules at nanometric resolution, creating an alternative solution to measure the mechanical properties of self-healing nanocapsules. As epoxy/catalyst self-healing system was the most straightforward system with simple fabrication process, scratch test was performed on the self-healing coating filled with epoxy microcapsules and Scandium (III) triflate ($Sc(OTf_3)$) catalyst on the metallic substrates. As scratch is performed, healing is triggered when the epoxy resin from the ruptured microcapsules reacts with the dispersed catalyst through ring-opening polymerization [8].

2. Experimental

2.1. Materials

Two types of epoxy resin (diglycidyl ether of bisphenol A) were used; EPIKOTE 828 (12,000–14,000 cps at 25 °C) as the epoxy matrix and ARALDITE 506 (500–700 cps at 25 °C) as the capsule core material. EPIKOTE 828 was purchased from ASACHEM (M) Sdn Bhd. ARALDITE 506, calcium chloride (analytical grade), glacial acetic acid (≥99.85%) and low molecular weight chitosan (50,000–190,000 DA, deacetylation degree of 75–85%) were purchased from Sigma-Aldrich. The hardener for epoxy matrix, diethylenetriamine (DETA) was purchased from BASF whereas halloysite nanotubes (Hallopure) was provided by i-Minerals (Canada). Sodium alginate (Manugel GHB, FMC Biopolymer, UK) with medium range molecular mass of 37% β-D-mannuronic acid (M) and 63% α-L-guluronic acid residues (G) was used in this study. The Scandium (III) triflate catalyst were procured from Fisher Scientific (M) Sdn Bhd.

2.2. Electrospraying method

Multicore AG/EPX microcapsules were produced through electrospraying as reported in the previous study [2]. Briefly, 2 w/v% of alginate solution was prepared by adding alginate into distilled water under mechanical mixing. The solution was then left overnight for degassing. Epoxy was gradually added into alginate solution during homogenization (IKA T10) at 1000 rpm for 30 min to form (5 v/v%) alginate/epoxy oil-in-water emulsion. Immediately, the emulsion was electrosprayed (10–15 kV) at a rate of 40 ml/hr into (2 w/v%) magnetic stirred grounded calcium chloride bath. The wet capsules were filtered and washed several times with distilled water before drying overnight at 45 °C.

2.3. Air atomization method

Another method, air atomization was employed to produce smaller size capsules. An air atomizer bottle was utilized to spray the epoxy/

Table 1
AG/EPX microcapsules fabricated under different conditions.

Samples	Fabrication Conditions				
	Electrospray	Air Atomization	HNTs (w/v%)	Chitosan[a] (w/v%)	Chitosan[b] (w/v%)
Espray-AG/EPX	✓				
Espray-AG/EPX/HNT(0.2)	✓		0.2		
Espray-AG/EPX/HNT(0.4)	✓		0.4		
Espray-AG/EPX/CTS(1)	✓			0.1	
Espray -AG/EPX/CTS(2)	✓			0.5	
Espray-AG/EPX/CTS(3)	✓			1	
Espray-AG/EPX/CTS(4)	✓				0.1
Espray-AG/EPX/CTS(5)	✓				0.5
Espray-AG/EPX/CTS(6)	✓				1
Air-AG/EPX		✓			
Air-AG/EPX/CTS(1)		✓		0.1	
Air-AG/EPX/CTS(2)		✓		0.5	
Air-AG/EPX/CTS(3)		✓		1	
Air-AG/EPX/CTS(4)		✓			0.1
Air-AG/EPX/CTS(5)		✓			0.5
Air-AG/EPX/CTS(6)		✓			1

[a] (Chitosan dissolving in 1 v/v % acetic acid).
[b] (Chitosan dissolving in 3 v/v % acetic acid).

alginate emulsion that was prepared into calcium chloride hardening bath. The air atomized bottle was kept 15 cm away and 15 cm above the hardening bath during spraying. The wet capsules formed were then sieved with mesh 20 to remove the clumps. The filtrate that contained AG/EPX capsules was then washed with distilled water for several times to remove excess calcium ions and dried overnight at 45 °C.

2.4. Chitosan coating

Chitosan solutions with various concentrations (0.1, 0.5 and 1.0 w/v%) were prepared by dissolving chitosan flakes into (1 and 3 v/v%) aqueous acetic acid solution. The mixture was magnetic stirred at 300 rpm for 2 h at room temperature. The chitosan solution was filtered to remove the undissolved chitosan flakes. Wet AG/EPX capsules (10 g) produced earlier using electrospraying and air atomization methods were suspended separately in 100 mL of chitosan solution for an hour. The capsules were then filtered and washed with distilled water before drying overnight at 45 °C. Table 1 shows the details of capsules produced.

2.5. HNTs incorporation

Halloysite nanotubes (HNTs) were incorporated into alginate solution by adding (0.2 and 0.4 w/v%) of HNTs into (2 w/v%) alginate solution and homogenized at 5000 rpm for 10 min followed by ultrasonic mixing (40 Hz) for 10 min while immersing in an ice bath. The solution was then mixed with epoxy to form epoxy/alginate emulsion and being electrosprayed to form HNTs modified AG/EPX microcapsules.

2.6. Capsule size and morphology

Capsule size analysis was performed using an Inverted Microscope (Nikon Eclipse Ti-U) and the size was measured using ImageJ software. The average diameter of the samples was analyzed from 200 measurements. Surface morphology and the cross section of the samples were analyzed by field emission scanning electron microscope (SEM) (SU8010 FE-SEM, Hitachi). The samples were coated with platinum for 30 s prior the analysis. For the cross-section analysis, the samples were embedded in epoxy matrix and being fractured. The fractured surface was rinsed with acetone to remove the encapsulated epoxy resin prior imaging.

2.7. Thermogravimetric analysis

Thermal stability of the samples was carried out through thermogravimetric analysis (TGA Q50, TA Instruments). The samples were heated up from 22 °C to 600 °C at a rate of 10 K/min under nitrogen atmosphere. Furthermore, the loading capacity (LC) of the microcapsules were determined to estimate the amount of epoxy resin being encapsulated using the formula below:

$$LC = \frac{W_1 - W_2}{1 - W_2} \quad (1)$$

where W_1 is the total weight loss of epoxy contained microcapsules and W_2 refers to total weight loss of the corresponding calcium alginate microcapsules obtained from TGA results [2,39]. For instance, to determine the LC of normal electrosprayed microcapsules, the corresponding W_2 refers to the pure calcium alginate microcapsules, whereas for chitosan coated AG/EPX microcapsules, the respective W_2 is based on chitosan coated calcium alginate microcapsules. For HNTs modified AG/EPX microcapsules, the corresponding W_2 is pure HNTs modified calcium alginate microcapsules.

2.8. Fourier transform infrared spectroscopy

Fourier transform infrared spectroscopy (FTIR) (Nicolet iS10 ATR-FTIR, ThermoFisher) was carried out to investigate the chemical structure of the samples at the range of 700–3700 cm^{-1} for the FTIR spectra. The tests were also carried out to confirm the presence of epoxy resin in the capsules.

2.9. Elastic modulus

Peak Force-QNM (PF-QNM) was performed using MultiMode 8 with Nanoscope V (Bruker, Germany) to study the topography (surface roughness) and nano-mechanical properties of the samples. All the measurements were carried out at ambient temperature. RTESP-300 and RTESP-525 cantilevers were used throughout the experiments with spring constant, $k = 200$ N/m and a nominal tip radius, $R = 8$ nm. Prior to the measurements, the cantilevers were calibrated through relative method as recommended by Bruker's user guide and the deflection sensitivity was measured on a glass surface based on an average value of three readings. Reference sample, polystyrene of known elastic modulus 2.7 GPa was used to calibrate the cantilevers. Subsequently,

acetone washed capsules were attached on the carbon tape before imaging. The Poisson's ratio was fixed at 0.4 for all the samples. The elastic modulus of the samples calculated through the Nanoscope software by fitting the force curve into Derjaguin-Muller-Toporov (DMT) model as shown below [40].

$$F - F_{adh} = \frac{4}{3}E^{*}\sqrt{R(d - d_0)^3} \quad (2)$$

$F - F_{adh}$ is the force on cantilever relative to adhesion force, E^{*} represents the reduced modulus, R is the tip end radius and $d - d_0$ is the sample deformation. Subsequently, the software will process the data to calculate elastic modulus based on the equation below.

$$E^{*} = \left[\frac{1 - \nu_s{}^2}{E_s} + \frac{1 - \nu_{tip}{}^2}{E_{tip}}\right]^{-1} \quad (3)$$

(ν_s, E_s) and (ν_{tip}, E_{tip}) represent the Poisson's ratio and elastic modulus of sample and tip. In this case, the elastic modulus of tip, E_{tip} is assumed to be infinite with the estimated value of (70–109 GPa) [41] and ν_{tip} to be 0.17. Since E_{tip} is much larger than elastic modulus of sample which means that the tip contribution can be neglected. Thus, the elastic modulus of the samples can be determined.

2.10. Self-healing epoxy coating

For the self-healing test, one type of microcapsule from each fabrication process (electrospraying and air atomization) were selected to produce the epoxy self-healing coatings to compare the self-healing ability with different microcapsule size. First, epoxy resin and DETA were mixed at the ratio of 100:12 which was used as the self-healing coating matrix. 10 wt% of modified AG/EPX microcapsules and 5 wt% of Sc(OTf_3) catalyst was then added into the epoxy resin and stirred homogeneously, followed by degassing. Iron plates (2 × 2 × 0.2 cm) were used as the metal substrate. Before coating, the metal substrates were treated with sandpaper and degreased with acetone, followed by applying the coating mixture using a brush. The thickness of the coatings was about 500 μm. Controlled samples without microcapsules were prepared in the same manner. All specimens were left overnight at room temperature to be fully cured prior going for further tests. For the self-healing test, the specimens were scratched with a scalpel and left overnight before characterizing with SEM to evaluate the self-healing performance.

3. Results and discussion

3.1. Microcapsules synthesis

Prior electrospraying and air atomization, epoxy was dispersed into alginate solution to form oil-in-water emulsion through the homogenizing procedure which reduced the epoxy droplet size within alginate solution. The emulsion was then undergone electrospraying and air atomization as shown in Fig. 1 to fabricate AG/EPX microcapsules. As shown in (Fig. 1b, e), both methods produce wet AG/EPX microcapsules encapsulated with multiple epoxy droplets. The main difference is the size of these wet microcapsules. The electrosprayed wet microcapsules have size bigger than 500 μm whereas air atomized wet microcapsules were below 200 μm. After drying, the electrosprayed microcapsules have an average diameter of 328 ± 3 μm (Fig. 1c) equipped with spherical shape and uneven surface. This is because when water evaporated from the wet capsules during the drying process, the capsules shrank, transforming the gel form beads to hardened capsules [2]. The size of the electrosprayed capsules is relatively large for self-healing coating applications. Moreover, most of the reported self-healing capsules are in the range of 10–200 μm [6,42,43]. Various parameters that could reduce the capsules size (< 150 μm) were investigated, such as alginate/epoxy emulsion volume flow rate, epoxy concentration, electric potential difference and concentration of alginate solution. Preliminary studies showed that the above-mentioned factors did not decrease the capsule size significantly except the epoxy/alginate emulsion volume flow rate. At a flow rate of 1 mL/h, capsules size below 100 μm was obtained. However, operating at this flow rate is ineffective and time-consuming.

Hence, air atomization was employed. Air atomization is an economical and simple technique that employs basic plumbing technique to operate an air atomizer bottle (Fig. 1d). As the pump presses down, air is being forced out of the nozzle that creates a quick drop in air pressure within the drawing tube near the pump. The higher atmospheric pressure in the bottle pushes the fluid into the drawing tube and out from the nozzle, creating fine liquid particles. Epoxy droplets were encapsulated within the air atomized wet capsules (Fig. 1e) with an average diameter of 126 ± 4 μm. However, these wet multicore microcapsules did not form spherical shape after drying. The dried air atomized microcapsules collapsed and aggregated with neighboring capsules (Fig. 1f). This can be explained by the heterogeneous structure of the capsules with denser polymer network on the capsule surface and softer core [44,45]. As the capsule size decreased, the amount of denser polymer network on outer surface decreased relatively, so when the capsules shrank as being dried, the pressure build up within the capsules raised and eventually the alginate polymer collapsed. Thus, methods to improve the structural integrity and mechanical strength of alginate matrix were sought.

3.2. Chitosan coating

The first modification method to enhance the structural integrity and mechanical properties of the unmodified electrosprayed and air atomized AG/EPX capsules was coated the wet AG/EPX microcapsules with chitosan polysaccharide before drying. The AG/EPX microcapsules were coated with chitosan that was dissolving in various acetic acid concentrations. As seen in (Fig. 2 a–b, d–e), chitosan coated electrosprayed microcapsules were found shrinking or even collapsing especially at low chitosan concentration (0.1, 0.5 w/v%). Most of the capsules were non-uniform associated with biconcave disc shape. In contrast, capsules coated with (1.0 w/v%) chitosan at both acetic acid concentration (Fig. 2c, f) were in spherical shape. However, at 3 v/v% acetic acid, the capsules surface was found to be smoother with thicker chitosan coating (Fig. 2f). This can be explained by the chitosan degree of protonation increases at higher acid concentration, therefore more chitosan were available to be coated on the capsules surface [46].

For air atomized microcapsules, coating with (0.1 w/v%) and (0.5 w/v%) chitosan did not provide significant improvements on the capsule rigidity as the capsules consistently found collapsed and coalesced (Fig. 2g–h, j–k). However, most of the capsules coated with (1.0 w/v%) chitosan appeared to be distinct capsules with irregular shape (Fig. 2i, l). This implied that (1.0 w/v%) would be the optimum amount of chitosan coated on the capsule surface to strengthen the alginate matrix and prevent it from collapsing. Our preliminary works confirmed that coating the air atomized microcapsules with more than 1.0 w/v% of chitosan resulted in collapsing structure too, which are not presented here. Thus, both electrosprayed and air atomized microcapsules coated with 1 w/v% chitosan dissolving in 3 v/v% acetic acid; Espray-AG/EPX/CTS(6) and Air-AG/EPX/CTS(6) were further studied on their respective physicochemical properties. Please refer Table 1 for the sample abbreviations.

3.3. HNTs incorporation

The second method to modify the capsules is by incorporating HNTs into alginate matrix. The HNTs was added into alginate polymer solution before mixing with epoxy and form microcapsules. The SEM images of dried unmodified and HNTs modified electrosprayed microcapsules were displayed (Fig. 3a–c). As compared to unmodified

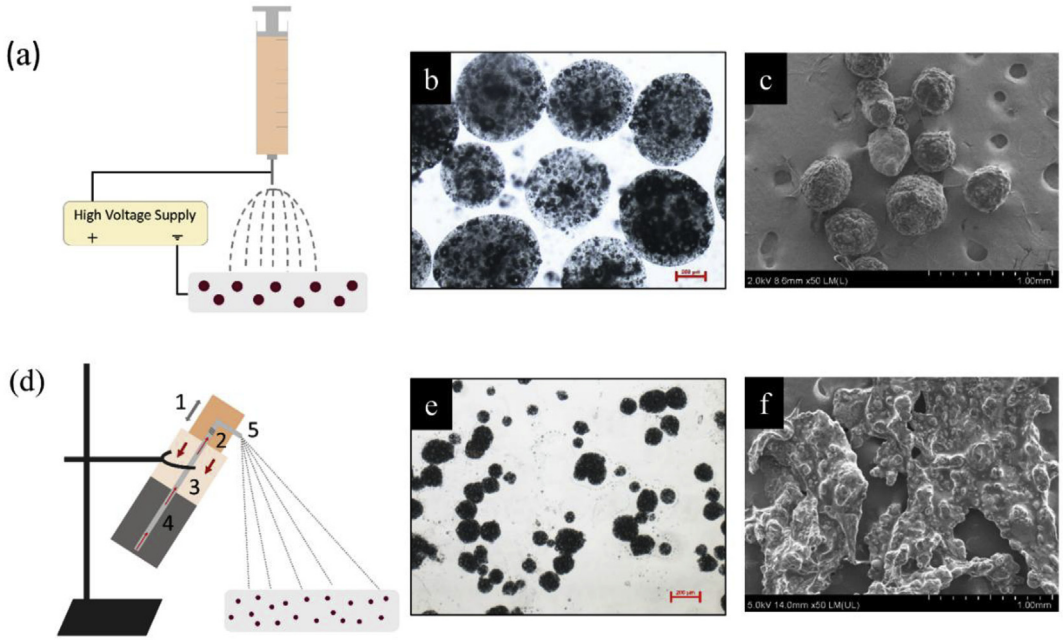

Fig. 1. Schematic of (a) electrospraying and (d) air atomization methods producing (b, e) multicore wet AG/EPX microcapsules with different capsule size. After drying overnight at 45 °C, (e) dried electrosprayed AG/EPX microcapsules were formed whereas the (f) air atomized microcapsules were collapsed. The scale bar of the images represent 200 μm (b,e) and 1 mm (c, f) respectively.

electrosprayed microcapsules, the size of HNTs modified microcapsules (Fig. 3b–c) was generally smaller and the shape was more irregular. Besides, holes were observed on the capsules surface on the HNTs modified microcapsules.

As mentioned earlier, air atomized microcapsules collapsed after drying due to its heterogeneous structure (Fig. 3d). Unfortunately, incorporating with HNTs did not successfully improved the collapsing issue for the air atomized microcapsules (Fig. 3e–f), collapsed polymer lumps were found at both 0.2 and 0.4 w/v% HNTs loading. This implied that incorporation of HNTs was not able to improve the structural integrity of alginate matrix for smaller microcapsules to form individual capsules after drying. This can be explained by the nature of HNTs which acts as nano-fillers that are attached physically instead of chemically bonded to the alginate matrix, thus it did not strengthen the weaker alginate polymer networks present in the core.

3.4. Capsule size and morphology

Both unmodified and modified AG/EPX microcapsules fabricated through electrospraying and air atomization were further studied on their surface morphology, cross-section and capsule size distribution (Fig. 4). As shown, all the samples were in spherical shape with uneven surface (Fig. 4a–e). The electrosprayed microcapsules that were coated with chitosan (Fig. 4b) have smoother surface compared to the normal electrosprayed capsules (Fig. 4a). Moreover, chitosan coating has also successfully strengthened the polymer network of smaller air atomized microcapsules (Fig. 4c), preventing the capsules collapsed during drying process. Adding of HNTs has affected the surface properties of the capsules as pores and dimples were developed on the surface of both Espray-AG/EPX/HNT(0.2) and Espray-AG/EPX/HNT(0.4) microcapsules (Fig. 4d and e). Moreover, some HNTs were found aligning parallel to the capsule surface, increasing the surface roughness of the microcapsules.

These microcapsules were then embedded into epoxy and the composite was fractured to study the internal structure. As shown, the chitosan coated microcapsules contained multicore internal structure (Fig. 4g–h). Comparatively, Air-AG/EPX/CTS(6) microcapsules (Fig. 4h) possessed fewer pores than the others due to smaller capsule size. Both chitosan coated samples showed good adhesion on epoxy matrix. Similarly, the HNTs modified electrosprayed microcapsules (Fig. 4i–j) possessed multicore internal structure. As the HNTs loading increased, there were fewer pores within the capsules and the wall between the pores were thicker [27]. On the submicron scale, it is great to notice that HNTs were homogeneously dispersed in alginate matrix which is important to yield a homogenous capsule in terms of mechanical properties that directly affect the homogeneity of the composite materials. Besides, both HNTs modified microcapsules showed good bonding with the epoxy matrix as well. At the broken alginate wall, HNTs were found unbroken and protruding from the alginate wall (Fig. 4n–o). In terms of alginate polymer thickness, the chitosan coated air atomized microcapsules, Air-AG/EPX/CTS(6) has the lowest polymer thickness at 1 μm as compared to others due to the smaller capsule size. The polymer thickness as shown might not represent the average value for these samples, but it gave an estimated value for the different microcapsules.

From the size distribution graphs, all the samples showed that their capsules sizes were normally distributed (Fig. 4p–t). Chitosan coating slightly decreased the electrosprayed microcapsules mean diameter from 328 ± 3 μm to 302 ± 3 μm as alginate shrank at low pH [47]. The mean diameter of chitosan coated air atomized microcapsules Air-AG/EPX/CTS(6) is 119 ± 3 μm which achieved the targeted size of (< 150 μm). For HNTs modified microcapsules, the mean diameter for both Espray-AG/EPX/HNT(0.2) and Espray-AG/EPX/HNT(0.4) were almost similar; 265 ± 3 μm and 255 ± 2 μm which were smaller than normal electrosprayed capsules. This could be explained by the fewer epoxy cores and thicker alginate matrix as seen in their internal structures.

3.5. Thermogravimetric analysis and loading capacity

The thermal behavior and epoxy loading capacity of different microcapsules were studied by TGA analysis (Fig. 5a). Referring to the TGA curve, the unmodified and chitosan modified microcapsules have very similar thermal decomposition profiles. The first 6–8% weight loss from 25 to 210 °C corresponded to the loss of adsorbed moisture and degradation of glycosidic bond while the second weight loss of about

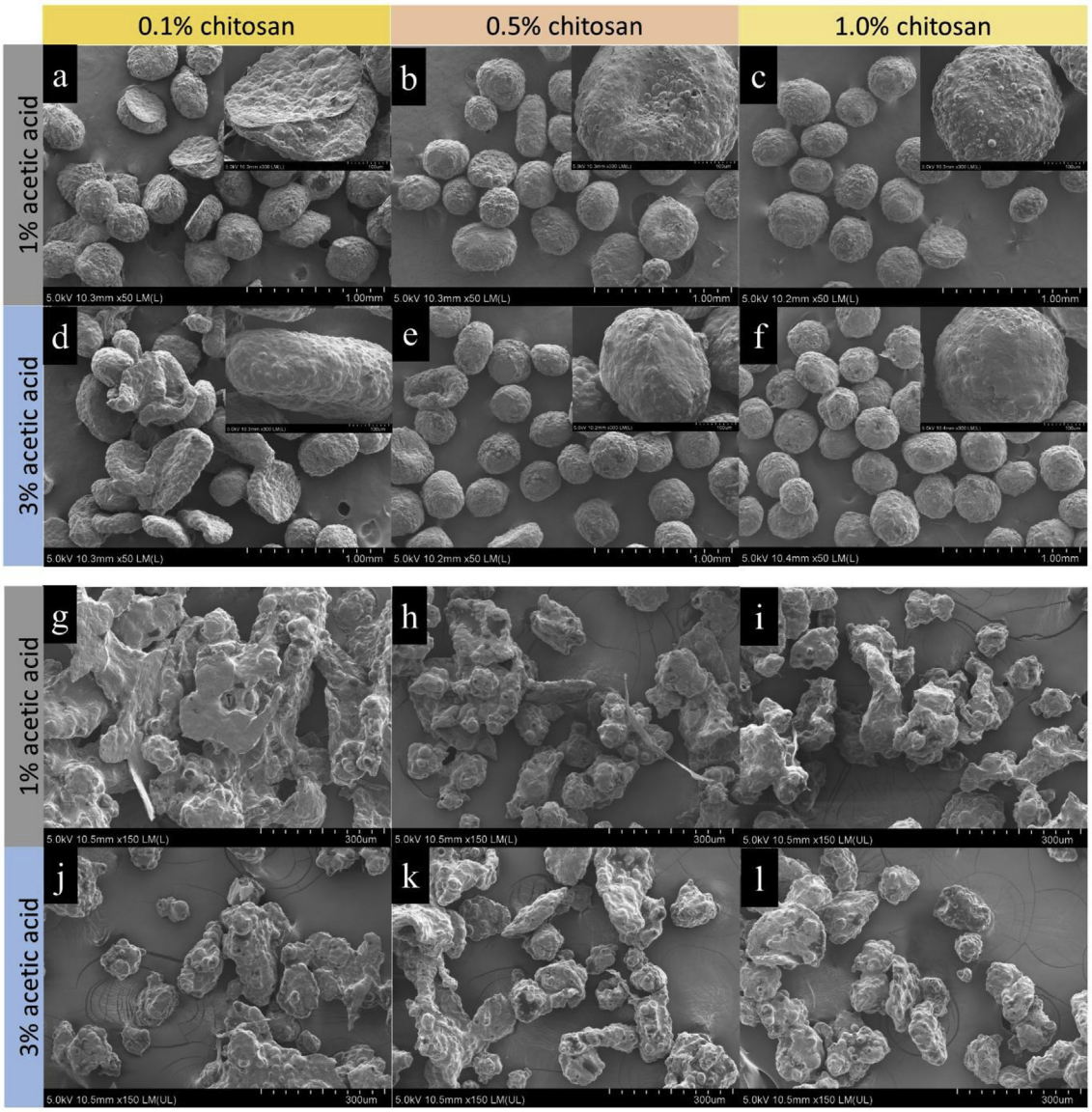

Fig. 2. SEM images of chitosan coated (a–f) electrosprayed microcapsules and (g–l) air atomized microcapsules. These microcapsules were coated at different chitosan concentration (0.1, 0.5, 1.0 w/v%) that were dissolving in (1, 3 v/v%) acetic acid.

50% from 210 to 350 °C was referred to the decomposition of encapsulated epoxy resin and further glycosidic bond mixture. The further weight loss was correspondent to the loss of residues of carbonaceous char and calcium carbonate [2]. Pure HNTs only started to decompose at 380 °C which was attributed to the dehydroxylation of structural Al-OH groups [48]. Adding 0.2 w/v% of HNTs did not give significant effect on the thermal stability of Espray-AG/EPX/HNT(0.2) microcapsules but at 0.4 w/v%, the thermal stability of Espray-AG/EPX/HNT(0.4) improved. For instance, to incur a 70% weight loss, the decomposition temperature increased from 375 °C for Espray-AG/EPX to 395 °C for Espray-AG/EPX/HNT(0.4). This indicates that HNTs modified microcapsules can be used for applications that require higher temperature tolerance.

The loading capacity of different microcapsules (Fig. 5b) was determined based on Equation (1). As shown, the loading capacity for the unmodified and modified microcapsules were close to each other ranging from 0.594 to 0.661 except for Espray-AG/EPX/HNT(0.4) where its LC was about 14% lower than Espray-AG/EPX. This could be explained by the holes appeared on the capsule surface of halloysite modified microcapsules (Fig. 4e), causing the leakage of encapsulated epoxy resin and lesser epoxy cores found in the capsules (Fig. 4j) which also indicates less epoxy content.

3.6. Fourier transform infrared spectroscopy

FTIR spectroscopy analysis was carried out for alginate, chitosan, normal and chitosan coated microcapsules (Fig. 6a). The FTIR spectrum of sodium alginate showed two distinct bands at 1593 cm^{-1} and 1409 cm^{-1} which were corresponded to carboxyl anions, COO^- (asymmetric and symmetric stretching vibrations) [49]. Chitosan showed weak band at 2873 cm^{-1} which corresponded to carbonyl C = O stretching of secondary amide (amide I band). The broad bands at 1652 cm^{-1} and 1589 cm^{-1} resembled the bending vibrations of N-H (N-acetylated residues) of amide I and amide II [50,51]. Subsequently, the bands 1418 cm^{-1} and 1374 cm^{-1} were corresponded to N-H stretching of amide and ether bonds and N-H stretching (amide III band). The distinctive bands of epoxy resin were shown at 3057 cm^{-1}, 1607 cm^{-1}, 1508 cm^{-1}, 1033 cm^{-1} and 915 cm^{-1}. The respective bands resembled to the stretching of C-H (oxirane ring), C = C (aromatic rings), C-C (aromatic), C-*O*-C (oxirane ethers) and C-O (oxirane group)

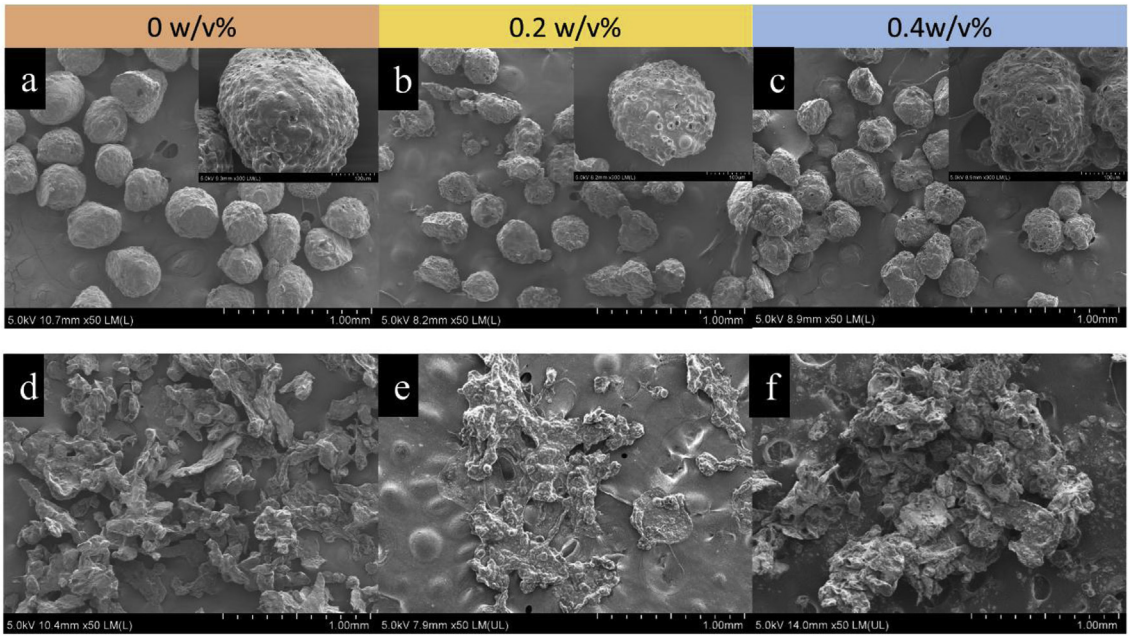

Fig. 3. SEM images of (a) electrosprayed and (b) collapsing air atomized microcapsules after drying overnight at 45 °C. HNTs modified (b–c) electrosprayed microcapsules and (f–g) air atomized microcapsules at different loadings (0.2, 0.4 w/v%).

[52]. Both Espray-AG/EPX and Espray-AG/EPX/CTS(6) showed distinct bands of epoxy resin which indicated the presence of epoxy resin within both types of capsules. Besides, a new band was observed at 1720 cm^{-1} for chitosan coated microcapsules, Espray-AG/EPX/CTS(6) which was referred to the protonation of carboxylate group in alginate [51].

The FTIR spectra of pure halloysite and halloysite modified microcapsules, Espray-AG/EPX/HNT(0.4) were studied (Fig. 6b). The main functional groups of halloysite consist of O-H stretching of inner-surface hydroxyl group at 3690 cm^{-1}, O-H stretching of inner hydroxyl groups at 3620 cm^{-1}, in-plane Si-O stretching at 1000 cm^{-1}, O-H deformation of inner hydroxyl groups at 908 cm^{-1}, symmetric and perpendicular stretching of Si-O at 792 cm^{-1} and 749 cm^{-1} [53]. After embedding HNTs into alginate, the bands at 3691 cm^{-1} and 3620 cm^{-1} that represent hydroxyl groups were found on Espray-AG/EPX/HNT(0.4) microcapsules. The respective Si-O stretching was found shifted towards 1010 cm^{-1}. Besides, the increase of intensity at band 912 cm^{-1} indicates the incorporation of HNTs into alginate matrix. The other bands found such as 1604 cm^{-1} (C=C, aromatic ring), 1508 cm^{-1} (C-C, aromatic), 1416 cm^{-1} (N-H stretching, ether) and 1027 cm^{-1} (C-*O*-C, oxirane ether) represented the presence of encapsulated epoxy resin. The absence of new bands could confirm that there was no chemical interaction between HNTs and alginate matrix as well as epoxy resin.

3.7. Surface topography and elastic modulus

The topography and the elastic modulus of unmodified and modified microcapsules were investigated using AFM through PF QNM mode. Height and the corresponding elastic modulus images were obtained with scan size of 1 × 1 μm for all samples (Fig. 7) and the average modulus for all the samples were calculated based on 3–6 measurements. The height images revealed the surface topography of the samples at nanoscopic scale. Coating of chitosan had no significant effect on the surface roughness of the microcapsules (Fig. 7c, e). The electrosprayed microcapsules, Espray-AG/EPX comprised of uniform circular alginate clusters (Fig. 7a) accompanied with roughness medium square (RMS) of 10.6 ± 3.1 nm [54]. Chitosan coated microcapsules presented irregular cluster (Fig. 7c, e) with RMS of 9.4 ± 1.0 nm and 10.4 ± 6.9 nm respectively. Chitosan coated electrosprayed microcapsules, Espray-AG/EPX/CTS(6) has elastic modulus of 4.45 ± 0.80 GPa which was higher than normal electrosprayed microcapsules at 3.43 ± 0.8 GPa. This implies that chitosan coating successfully binds onto alginate wall while improving the mechanical strength of microcapsules. However, smaller size chitosan coated air atomized microcapsules have lower elastic modulus of 2.05 ± 0.30 GPa. This is due to the thinner alginate matrix (Fig. 4m) associated with smaller capsules and thus the amount of load that it can withstand is decreasing. Similar behavior was also found on poly-melamine formaldehyde (PMF) self-healing microcapsules [55,56].

For the HNTs modified microcapsules, both samples showed rod-like structure in the height images (Fig. 7g, i) that corresponded to HNTs. In addition, alginate patches were noticed on top of HNTs, indicating a homogeneous incorporation of HNTs within the alginate matrix. These HNTs modified microcapsules were associated with RMS of 26.5.1 ± 23.1 nm and 13.3 ± 1.4 nm respectively. Both samples have higher surface roughness as compared to normal electrosprayed microcapsules as there were two different phases contained; HNTs and calcium alginate polymer. Increasing the HNTs loading from 0.2 w/v% to 0.4 w/v% increased the elastic modulus of the microcapsules from 4.71 ± 1.46 GPa to 6.04 ± 0.20 GPa. To date, studies have done on assessing the mechanical properties of self-healing microcapsules using nanoindentation method where the interaction between tip and polymer is not taken into account [57]. The corresponded elastic modulus for these capsules is in the range of 2.70–4.60 GPa with capsule size of 5–160 μm [55,56,58]. Besides, the capsule elastic modulus increased with size and incorporation of nanoparticles [58]. As a comparison, the unmodified and modified AG/EPX microcapsules were having an elastic modulus of 2.0–6.0 GPa. This indicates that the mechanical properties of alginate biopolymer self-healing microcapsules are comparable with the reported organic polymer self-healing microcapsules. Furthermore, at this range of elastic modulus, these AG/EPX microcapsules should be able to retain its structure during preparation of self-healing composites.

3.8. Self-healing coating

Our previous study shows that samples filled with unmodified electrosprayed AG/EPX microcapsules and catalyst were able to perform multiple healing [59]. In this study, the capsule-catalyst self-

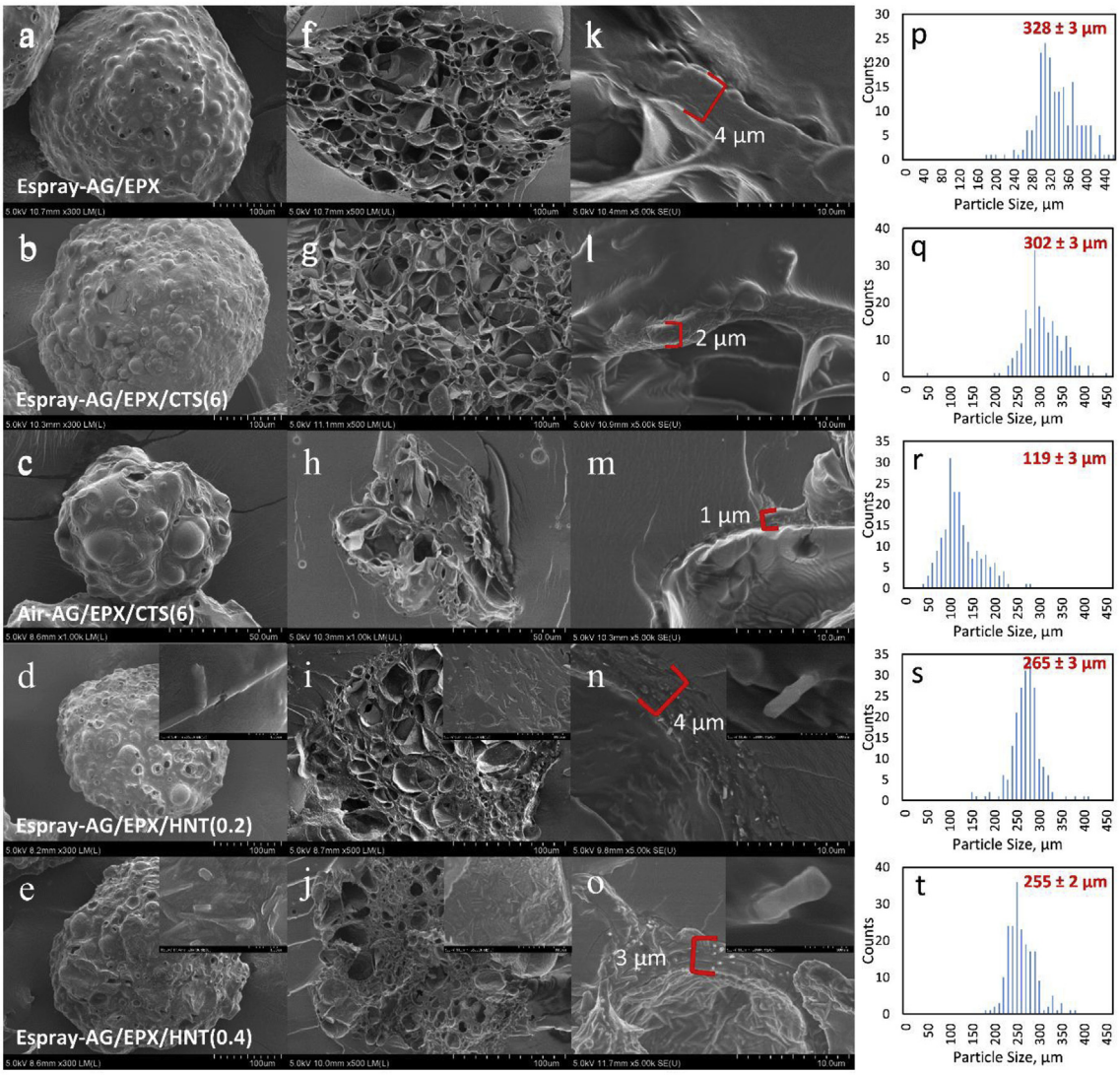

Fig. 4. (a–e) Capsule surface morphology, (f–j) cross section, (h–o) alginate polymer thickness and the (p–t) particle size distribution for electrosprayed microcapsules (Espray-AG/EPX), chitosan coated microcapsules (Espray-AG/EPX/CTS(6)), air atomized microcapsules (Air-AG/EPX/CTS(6)) and HNTs modified microcapsules [Espray-AG/EPX/HNT(0.2) & Espray-AG/EPX/HNT(0.4)].

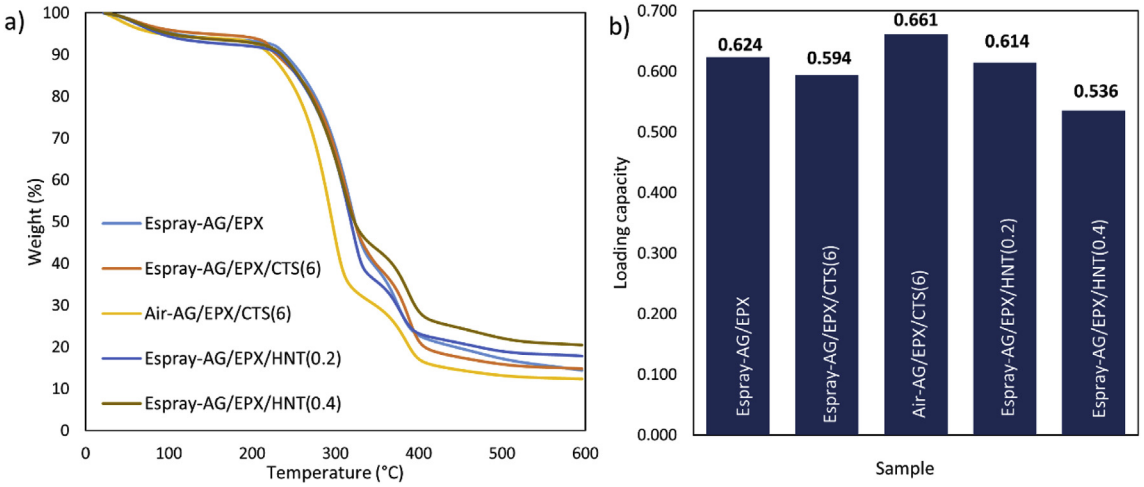

Fig. 5. (a) TGA curve of unmodified and modified AG/EPX microcapsules with their (b) loading capacity.

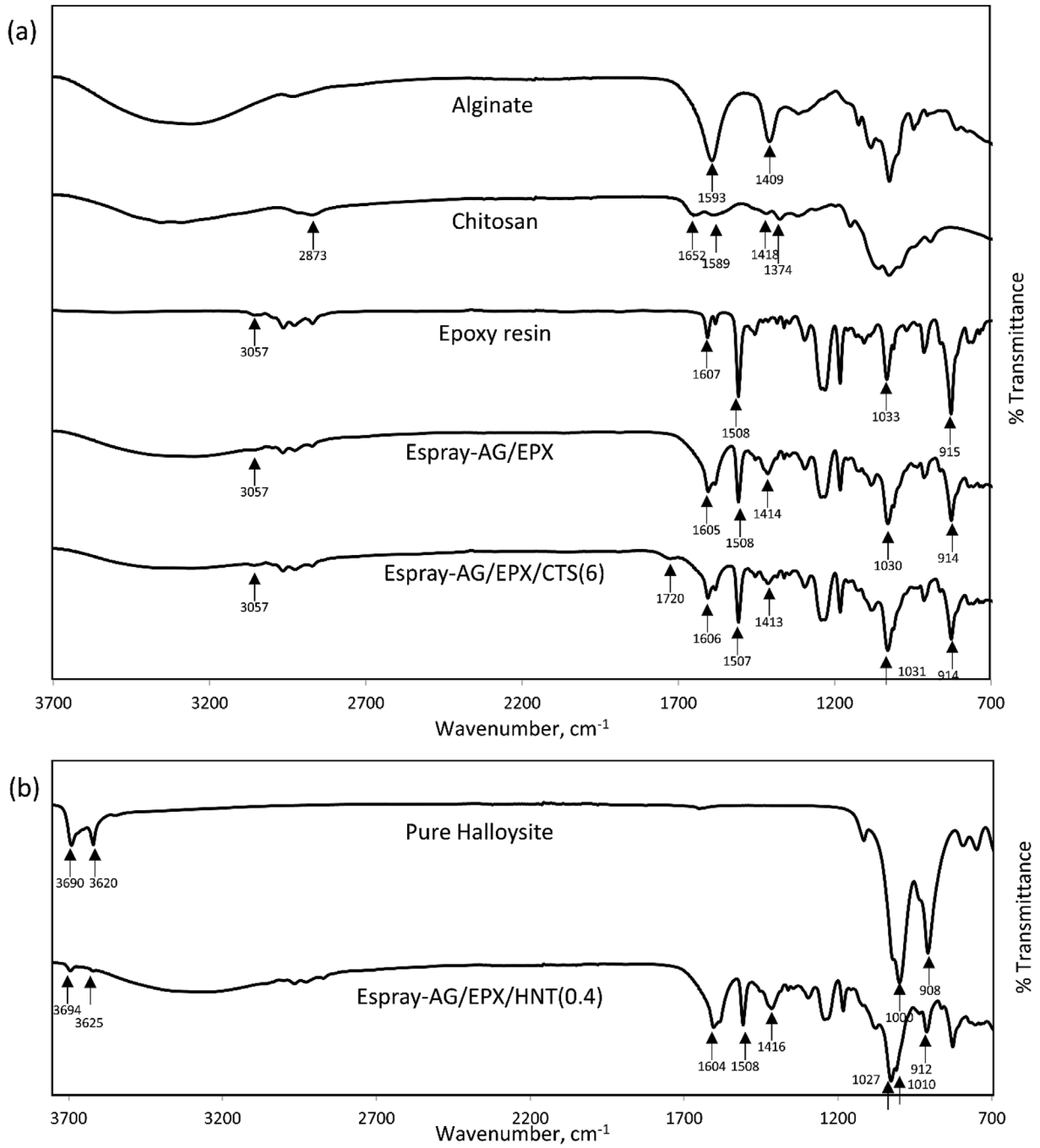

Fig. 6. FTIR spectra of (a) alginate, chitosan, epoxy resin (Araldite 506), electrosprayed (E-spray-AG/EPX) and chitosan coated microcapsules (Espray-AG/EPX/CTS (6)) followed by (b) pure halloysite (Hallopure) and halloysite modified microcapsules (Espray-AG/EPX/HNT(0.4)).

healing coating was fabricated by embedding 10 wt% modified AG/EPX microcapsules with two different size ranges (~150 μm and ~350 μm) and 5 wt% solid catalyst, $Sc(OTf_3)$ into epoxy resin matrix. The capsules that were used to perform the test were the chitosan coated air atomized microcapsules (Air-AG/EPX/CTS(6)) and HNTs modified electrosprayed microcapsules (E-spray-AG/EPX/HNT(0.4)). The self-healing epoxy mixture was then applied on metal plates and scratch tests were performed. As shown in Fig. 8a, the controlled specimen associated with a scratch (width: ca. 30 μm, depth: ca. 40 μm) perceived no signs of healing as the depth of the scratch was clearly seen. On the other hand, both the scratches in the self-healing coatings with modified AG/EPX microcapsules showed signs of healing as the scratches were being filled up by the healing agents (Fig. 8b–c). Adding HNTs did not hindered the releasing of epoxy resin from the microcapsules. As the coating were damaged, the capsules along the scratch were broken, releasing epoxy resin into the cavities and undergo ring-opening polymerization with the catalyst, thus filling up the gap. However, the damage in the self-healing coating filled with smaller microcapsules (Fig. 8b) was not fully covered as a small cavity was noticed at the end of the scratch. The low coverage of healing agents can be explained by the smaller capsule size which has less healing agents available to heal a similar damage as compared to bigger microcapsules. Overall, this test proved the self-healing ability of multicore AG/EPX microcapsules with varied sizes in healing the microcracks.

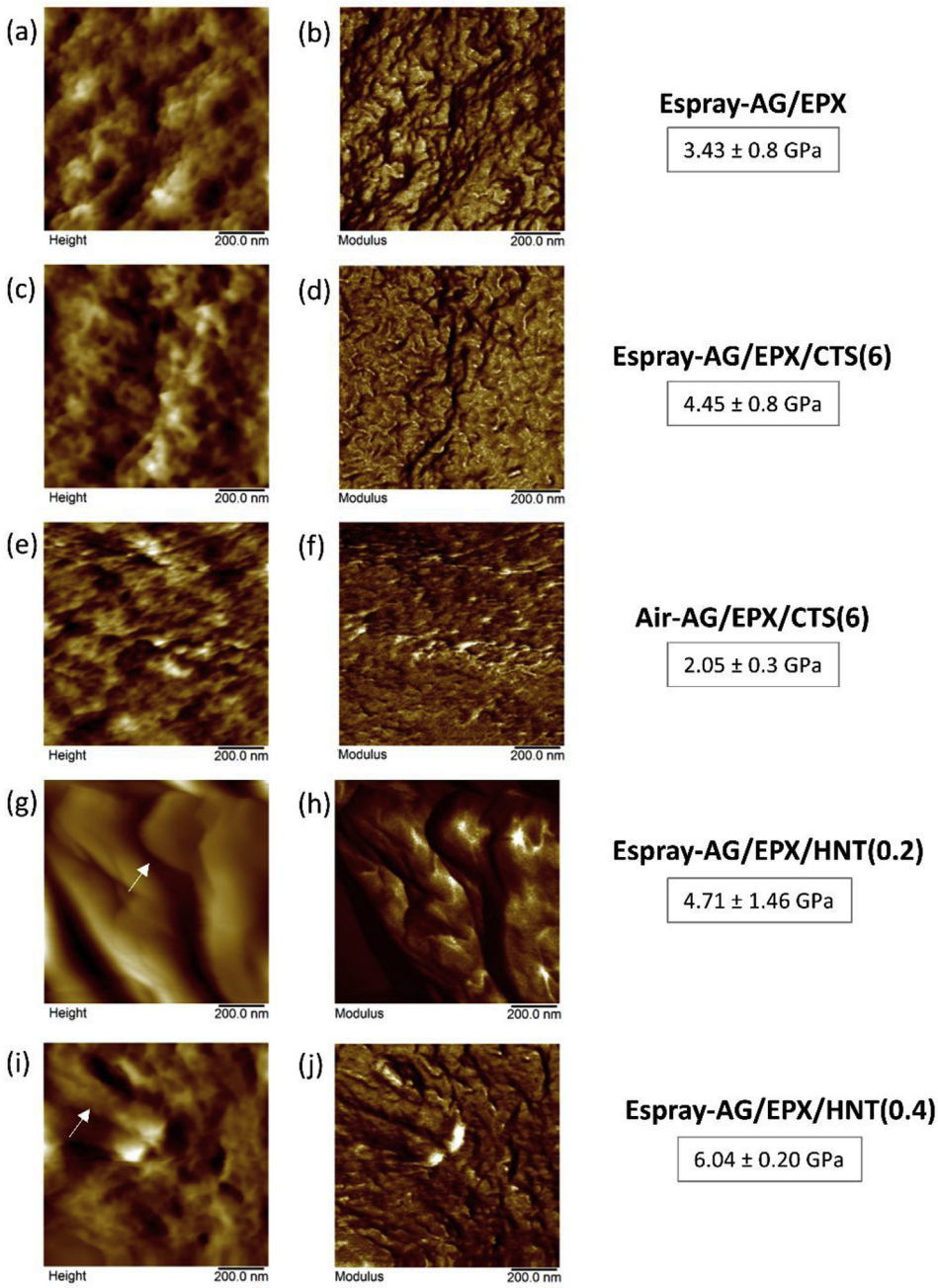

Fig. 7. Height and elastic modulus images of (a–b) electrosprayed microcapsules, (c–d) chitosan coated electrosprayed microcapsules, (e–f) chitosan coated air atomized microcapsules and (g–j) HNTs modified electrosprayed microcapsules as obtained from Peak force QNM mode. The scan size for all samples are in 1 μm × 1 μm.

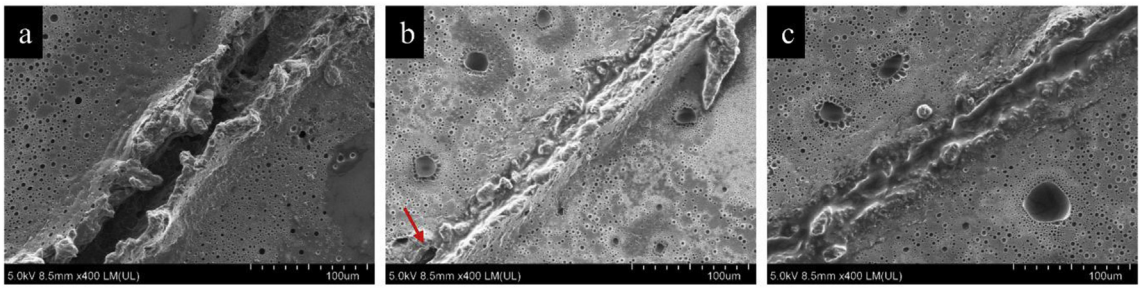

Fig. 8. Scratch test on the epoxy coating (a) without any microcapsules and self-healing coating loaded with 10 wt% of (b) small chitosan coated air atomized microcapsules (Air-AG/EPX/CTS(6)) and (c) big electrosprayed HNTs modified microcapsules (Espray-AG/EPX/HNT(0.4)) along with 5 wt %$Sc(OTf_3)$ catalyst.

4. Conclusions

In this study, facile methods were developed to produce green self-healing epoxy microcapsules in two size range (< 150 μm and > 300 μm). These fabrication processes are much simpler and economical as compared to other self-healing microcapsules as reported in the literature. Chitosan coating providentially improved the structural integrity of the small capsules. Besides, the elastic modulus of chitosan coated microcapsules increased by 30% as compared to normal electrosprayed microcapsules. This work shows that chitosan coating is a promising way to enhance the structural integrity and mechanical properties of alginate self-healing microcapsules at both large and small sizes. The chitosan coated self-healing microcapsules with higher elastic modulus not cater to enhance the mechanical properties of the composites, but also for different potential applications from thick concrete materials to thin coatings. In contrast, incorporation of HNTs did not provide structural support to the smaller capsules but it enhanced the thermal properties and increased the elastic modulus by 76% for the bigger microcapsules. It is believed that the improved thermal and mechanical properties of HNTs modified microcapsules can sustain better in harsh processing environment of self-healing composite. Besides, microcapsules with higher elastic modulus are expected to improve the coating mechanical properties. On the other hand, the self-healing performance of these microcapsules were evaluated through scratch test in the self-healing coatings. Those self-healing coatings that filled with microcapsules with varied sizes and catalyst showed signs of healing by closing the gaps of the scratches. Future works may focus on the mechanical properties (hardness, elastic modulus, interfacial fracture toughness) and further evaluation on the self-healing performance (anticorrosion and electrochemical testing) of the coating filled with modified AG/EPX microcapsules.

Acknowledgement

The authors would like to acknowledge Ministry of Higher Education Malaysia for supporting this research under FRGS/2/2013/TK04/MUSM/03/1, Monash University for the PhD scholarship.

References

[1] E.N. Brown, S.R. White, N.R. Sottos, Microcapsule induced toughening in a self-healing polymer composite, J. Mater. Sci. 39 (2004) 1703–1710.
[2] I.L. Hia, P. Pasbakhsh, E.-S. Chan, S.-P. Chai, Electrosprayed multi-core alginate microcapsules as novel self-healing containers, Sci. Rep. 6 (2016) 34674.
[3] D. Therriault, S.R. White, J.A. Lewis, Chaotic mixing in three-dimensional microvascular networks fabricated by direct-write assembly, Nat. Mater. 2 (2003) 265–271.
[4] K. Toohey, N. Sottos, S. White, Characterization of microvascular-based self-healing coatings, Exp. Mech. 49 (2009) 707–717.
[5] V. Vahedi, P. Pasbakhsh, C.S. Piao, C.E. Seng, A facile method for preparation of self-healing epoxy composites: using electrospun nanofibers as microchannels, J. Mater. Chem. A 3 (2015) 16005–16012.
[6] S.R. White, N.R. Sottos, P.H. Geubelle, J.S. Moore, M.R. Kessler, S.R. Sriram, E.N. Brown, S. Viswanathan, Autonomic healing of polymer composites, Nature 409 (2001) 794–797.
[7] J.M. Kamphaus, J.D. Rule, J.S. Moore, N.R. Sottos, S.R. White, A new self-healing epoxy with tungsten (VI) chloride catalyst, J. R. Soc. Interface 5 (2008) 95–103.
[8] T.S. Coope, U.F.J. Mayer, D.F. Wass, R.S. Trask, I.P. Bond, Self-healing of an epoxy resin using Scandium(III) triflate as a catalytic curing agent, Adv. Funct. Mater. 21 (2011) 4624–4631.
[9] L. Guadagno, M. Raimondo, C. Naddeo, P. Longo, A. Mariconda, Self-healing materials for structural applications, Polym. Eng. Sci. 54 (2014) 777–784.
[10] Y.C. Yuan, M.Z. Rong, M.Q. Zhang, J. Chen, G.C. Yang, X.M. Li, Self-healing polymeric materials using epoxy/mercaptan as the healant, Macromolecules 41 (2008) 5197–5202.
[11] H. Zhang, J. Yang, Etched glass bubbles as robust micro-containers for self-healing materials, J. Mater. Chem. A 1 (2013) 12715–12720.
[12] X.K. Hillewaere, R.F. Teixeira, L.T.T. Nguyen, J.A. Ramos, H. Rahier, F.E. Du Prez, Autonomous self-healing of epoxy thermosets with thiol-isocyanate chemistry, Adv. Funct. Mater. 24 (2014) 5575–5583.
[13] M. Xie, L. Wang, F. Liu, D. Zhang, J. Gao, Dynamic conversion between Se–N covalent and noncovalent interactions, J. Phys. Chem. A 120 (2016) 9081–9088.
[14] R. Zhang, S. Yu, S. Chen, Q. Wu, T. Chen, P. Sun, B. Li, D. Ding, Reversible cross-linking, microdomain structure, and heterogeneous dynamics in thermally reversible cross-linked polyurethane as revealed by solid-state NMR, J. Phys. Chem. B 118 (2014) 1126–1137.
[15] M. Huang, J. Yang, Facile microencapsulation of HDI for self-healing anticorrosion coatings, J. Mater. Chem. 21 (2011) 11123–11130.
[16] C. Suryanarayana, K.C. Rao, D. Kumar, Preparation and characterization of microcapsules containing linseed oil and its use in self-healing coatings, Prog. Org. Coat. 63 (2008) 72–78.
[17] G.L. Li, M. Schenderlein, Y. Men, H. Möhwald, D.G. Shchukin, Monodisperse polymeric core–shell nanocontainers for organic self-healing anticorrosion coatings, Adv. Mater. Interfaces 1 (2014).
[18] H. Yi, Y. Yang, X. Gu, J. Huang, C. Wang, Multilayer composite microcapsules synthesized by Pickering emulsion templates and their application in self-healing coating, J. Mater. Chem. A 3 (2015) 13749–13757.
[19] A.E. Hughes, I.S. Cole, T.H. Muster, R.J. Varley, Designing green, self-healing coatings for metal protection, NPG Asia Mater. 2 (2010) 143.
[20] M. Samadzadeh, S.H. Boura, M. Peikari, A. Ashrafi, M. Kasiriha, Tung oil: an autonomous repairing agent for self-healing epoxy coatings, Prog. Org. Coat. 70 (2011) 383–387.
[21] E. Koh, S.-Y. Baek, N.-K. Kim, S. Lee, J. Shin, Y.-W. Kim, Microencapsulation of the triazole derivative for self-healing anticorrosion coatings, New J. Chem. 38 (2014) 4409–4419.
[22] H. Yi, Y. Deng, C. Wang, Pickering emulsion-based fabrication of epoxy and amine microcapsules for dual core self-healing coating, Compos. Sci. Technol. 133 (2016) 51–59.
[23] S.H. Cho, S.R. White, P.V. Braun, Self-healing polymer coatings, Adv. Mater. 21 (2009) 645–649.
[24] I.L. Hia, V. Vahedi, P. Pasbakhsh, Self-healing polymer composites: prospects, challenges, and applications, Polym. Rev. 56 (2016) 225–261.
[25] Z. Ahmad, G.K. Khuller, Alginate-based sustained release drug delivery systems for tuberculosis, Expet Opin. Drug Deliv. 5 (2008) 1323.
[26] M. Balyura, E. Gelfgat, M. Ehrhart-Bornstein, B. Ludwig, Z. Gendler, U. Barkai, B. Zimerman, A. Rotem, N.L. Block, A.V. Schally, S.R. Bornstein, Transplantation of bovine adrenocortical cells encapsulated in alginate, Proc. Natl. Acad. Sci. U.S.A. 112 (2015) 2527.
[27] C.S.C. Chiew, P.E. Poh, P. Pasbakhsh, B.T. Tey, H.K. Yeoh, E.S. Chan, Physicochemical characterization of halloysite/alginate bionanocomposite hydrogel, Appl. Clay Sci. 101 (2014) 444–454.
[28] O. Smidsrød, G. Skja, Alginate as immobilization matrix for cells, Trends Biotechnol. 8 (1990) 71–78.
[29] J. Shi, N.M. Alves, J.F. Mano, Chitosan coated alginate beads containing poly (N-isopropylacrylamide) for dual-stimuli-responsive drug release, J. Biomed. Mater. Res. B Appl. Biomater. 84 (2008) 595–603.
[30] O. Gåserød, A. Sannes, G. Skjåk-Bræk, Microcapsules of alginate–chitosan. II. A study of capsule stability and permeability, Biomaterials 20 (1999) 773–783.
[31] O. Gåserød, O. Smidsrød, G. Skjåk-Bræk, Microcapsules of alginate-chitosan–I: a quantitative study of the interaction between alginate and chitosan, Biomaterials 19 (1998) 1815–1825.
[32] S. Rooj, A. Das, G. Heinrich, Tube-like natural halloysite/fluoroelastomer nanocomposites with simultaneous enhanced mechanical, dynamic mechanical and thermal properties, Eur. Polym. J. 47 (2011) 1746–1755.
[33] B. Lecouvet, M. Sclavons, S. Bourbigot, J. Devaux, C. Bailly, Water-assisted extrusion as a novel processing route to prepare polypropylene/halloysite nanotube nanocomposites: structure and properties, Polymer 52 (2011) 4284–4295.
[34] M. Liu, Y. Zhang, C. Zhou, Nanocomposites of halloysite and polylactide, Appl. Clay Sci. 75–76 (2013) 52–59.
[35] R. De Silva, P. Pasbakhsh, K. Goh, S.-P. Chai, H. Ismail, Physico-chemical characterisation of chitosan/halloysite composite membranes, Polym. Test. 32 (2013) 265–271.
[36] P. Pasbakhsh, G.J. Churchman, J.L. Keeling, Characterisation of properties of various halloysites relevant to their use as nanotubes and microfibre fillers, Appl. Clay Sci. 74 (2013) 47–57.
[37] B. Lecouvet, J. Horion, C. D'Haese, C. Bailly, B. Nysten, Elastic modulus of halloysite nanotubes, Nanotechnology 24 (2013) 105704.
[38] M. Liu, Z. Jia, D. Jia, C. Zhou, Recent advance in research on halloysite nanotubes-polymer nanocomposite, Prog. Polym. Sci. 39 (2014) 1498–1525.
[39] C. Liu, B. Liang, G. Shi, Z. Li, X. Zheng, Y. Huang, L. Lin, Preparation and characteristics of nanocapsules containing essential oil for textile application, Flavour Fragrance J. 30 (2015) 295–301.
[40] B. Pittenger, N. Erina, C. Su, Quantitative Mechanical Property Mapping at the Nanoscale with PeakForce QNM, Application Note Veeco Instruments Inc, 2010.
[41] G. Smolyakov, S. Pruvost, L. Cardoso, B. Alonso, E. Belamie, J. Duchet-Rumeau, AFM PeakForce QNM mode: evidencing nanometre-scale mechanical properties of chitin-silica hybrid nanocomposites, Carbohydr. Polym. 151 (2016) 373–380.
[42] H. Jin, G.M. Miller, S.J. Pety, A.S. Griffin, D.S. Stradley, D. Roach, N.R. Sottos, S.R. White, Fracture behavior of a self-healing, toughened epoxy adhesive, Int. J. Adhes. Adhes. 44 (2013) 157–165.
[43] Y.C. Yuan, M.Z. Rong, M.Q. Zhang, G.C. Yang, Study of factors related to performance improvement of self-healing epoxy based on dual encapsulated healant, Polymer 50 (2009) 5771–5781.
[44] J. Lee, D. Cha, H.J. Park, Survival of freeze-dried Lactobacillus bulgaricus KFRI 673 in chitosan-coated calcium alginate microparticles, J. Agric. Food Chem. 52 (2004) 7300–7305.
[45] G. Skjåk-Bræk, H. Grasdalen, O. Smidsrød, Inhomogeneous polysaccharide ionic gels, Carbohydr. Polym. 10 (1989) 31–54.
[46] M. Rinaudo, G. Pavlov, J. Desbrières, Influence of acetic acid concentration on the

solubilization of chitosan, Polymer 40 (1999) 7029–7032.
[47] S.-C. Chen, Y.-C. Wu, F.-L. Mi, Y.-H. Lin, L.-C. Yu, H.-W. Sung, A novel pH-sensitive hydrogel composed of N,O-carboxymethyl chitosan and alginate cross-linked by genipin for protein drug delivery, J. Contr. Release 96 (2004) 285–300.
[48] P. Sun, G. Liu, D. Lv, X. Dong, J. Wu, D. Wang, Effective activation of halloysite nanotubes by piranha solution for amine modification via silane coupling chemistry, RSC Adv. 5 (2015) 52916–52925.
[49] M.G. Sankalia, R.C. Mashru, J.M. Sankalia, V.B. Sutariya, Reversed chitosan–alginate polyelectrolyte complex for stability improvement of alpha-amylase: optimization and physicochemical characterization, Eur. J. Pharm. Biopharm. 65 (2007) 215–232.
[50] Y.-N. Dai, P. Li, J.-P. Zhang, A.-Q. Wang, Q. Wei, Swelling characteristics and drug delivery properties of nifedipine-loaded pH sensitive alginate–chitosan hydrogel beads, J. Biomed. Mater. Res. B Appl. Biomater. 86B (2008) 493–500.
[51] G. Lawrie, I. Keen, B. Drew, A. Chandler-Temple, L. Rintoul, P. Fredericks, L. Grøndahl, Interactions between alginate and chitosan biopolymers characterized using FTIR and XPS, Biomacromolecules 8 (2007) 2533–2541.
[52] M.G. González, J. Baselga, J.C. Cabanelas, Applications of FTIR on Epoxy Resins-identification, Monitoring the Curing Process, Phase Separation and Water Uptake, Intech Open Access Publisher, 2012.
[53] P. Yuan, P.D. Southon, Z. Liu, M.E.R. Green, J.M. Hook, S.J. Antill, C.J. Kepert, Functionalization of halloysite clay nanotubes by grafting with γ-aminopropyltriethoxysilane, J. Phys. Chem. C 112 (2008) 15742–15751.
[54] G. Carturan, R. Dal Toso, S. Boninsegna, R. Dal Monte, Encapsulation of functional cells by sol-gel silica: actual progress and perspectives for cell therapy, J. Mater. Chem. 14 (2004) 2087–2098.
[55] J.-F. Su, X.-Y. Wang, H. Dong, Micromechanical properties of melamine–-formaldehyde microcapsules by nanoindentation: effect of size and shell thickness, Mater. Lett. 89 (2012) 1–4.
[56] J. Lee, M. Zhang, D. Bhattacharyya, Y.C. Yuan, K. Jayaraman, Y.W. Mai, Micromechanical behavior of self-healing epoxy and hardener-loaded microcapsules by nanoindentation, Mater. Lett. 76 (2012) 62–65.
[57] M. Griepentrog, G. Krämer, B. Cappella, Comparison of nanoindentation and AFM methods for the determination of mechanical properties of polymers, Polym. Test. 32 (2013) 455–460.
[58] M. Ghorbanzadeh Ahangari, A. Fereidoon, M. Jahanshahi, N. Sharifi, Effect of nanoparticles on the micromechanical and surface properties of poly(urea–formaldehyde) composite microcapsules, Compos. B Eng. 56 (2014) 450–455.
[59] I.L. Hia, E.-S. Chan, S.-P. Chai, P. Pasbakhsh, A novel repeated self-healing epoxy composite with alginate multicore microcapsules, J. Mater. Chem. A (2018), http://dx.doi.org/10.1039/C8TA01783B.